Preprints (www.preprints.org) | NOT PEER-REVIEWED | Posted: 29 February 2020 doi:10.20944/preprints202002.0464.v1

Peer-reviewed version available at *Materials* **2020**, *13*, 1428; doi:10.3390/ma13061428

$C_{0.3}N_{0.7}$Ti-SiC toughed silicon nitride hybrids with non-oxide additives Ti_3SiC_2

Heng Luo[1*], Chen Li[1], Lianwen Deng[1], Yang Li[2], Peng Xiao[2], Haibin Zhang[3]

1. School of Physics and Electronics, Central South University, Changsha, 410083, China

2. State Key Laboratory of Powder Metallurgy, Central South University, Changsha 410083, China

3. Innovation Research Team for Advanced Ceramics, Institute of Nuclear Physics and Chemistry, China Academy of Engineering Physics, Mianyang, 621900, China

Abstract: *In-situ* grown $C_{0.3}N_{0.7}$Ti and SiC, which derived from non-oxide additives Ti_3SiC_2, are proposed to densify silicon nitride (Si_3N_4) ceramics with enhanced mechanical performance. Remarkable increase of density from 79.20% to 95.48% could be achieved for Si_3N_4 ceramics with 5vol% Ti_3SiC_2. The capillarity of decomposed Si from Ti_3SiC_2, and *in-situ* reaction between nonstoichiometric TiC_x and Si_3N_4 were believed to be responsible for densification of Si_3N_4 ceramics. An obvious enhancement of flexural strength and fracture toughness for Ti_3SiC_2 doped Si_3N_4 ceramics was observed. The maximum flexural strength of 795 MPa for Si_3N_4 composites with 5vol% Ti_3SiC_2 and maximum fracture toughness of 6.97 $MPa{\cdot}m^{1/2}$ for Si_3N_4 composites with 20vol% Ti_3SiC_2 are achieved when mixed powders are hot-press sintered at 1700℃. Pull out of elongated Si_3N_4 grains, crack bridging, crack branching and crack deflection were demonstrated to dominate enhance fracture toughness of Si_3N_4 composites.

Keywords: Ti_3SiC_2; Si_3N_4; mechanical properties; fracture toughness

1. Introduction

Although a number of alternatives of structural ceramics have been proposed, silicon nitride (Si_3N_4)-based ceramics remain competitive due to their superior properties, involving high strength and hardness at elevated temperatures, high resistance to oxidation and chemical attack, low coefficient of tribological friction and thermal expansion, and low dielectric permittivity, etc. [1-9]. As important multifunctional materials, Si_3N_4 ceramics have found wide range of successful application towards gas turbine engine components [10-13], cutting tools [10, 14], radomes [2], and even integrated circuit [15, 16], optical devices [17, 18], etc.

However, due to the high degree of covalent bonding, Si_3N_4-based ceramics are very difficult to densify through the solid-state sintering process. Therefore, effective approaches to ensure rapid consolidation and high mechanical performance of Si_3N_4-based ceramics are actively being explored, including gas pressure sintering (GPS)[10], hot-pressing sintering (HPS)[19-25], hot isostatic pressing sintering (HIP)[26], spark plasma sintering (SPS)[25, 27, 28], and microwave sintering [1, 29], etc. However, considering the requirement of high gas pressures for gas pressure sintering and extra current devices for SPS with a significantly higher furnace costs, HP sintering allows the dense and complex-shaped parts with medium cost. Previous considerable efforts have demonstrated that fully dense Si_3N_4 ceramics with superior strength could be achieved through liquid phase sintering by addition of rare-earth oxides to promote mass transport and accelerate the rate of $\alpha-\beta$ transformation, most notably the rare-earth oxides involving Y_2O_3 [4, 30, 31]. A combination of various rare-earth oxides

* Corresponding authors. Email: luohengcsu@csu.edu.cn (H. Luo). Address: School of Physics and Electronics, Central South University, Changsha, 410083, P.R. China.

Preprints (www.preprints.org) | NOT PEER-REVIEWED | Posted: 29 February 2020 doi:10.20944/preprints202002.0464.v1

Peer-reviewed version available at Materials 2020, 13, 1428; doi:10.3390/ma13061428

and other metallic oxides, such as Y_2O_3, La_2O_3, Nd_2O_3, Sm_2O_3, Yb_2O_3, Lu_2O_3, Al_2O_3 and MgO, also are effective sintering aids to densify Si_3N_4 [24, 29, 31-34].
Nevertheless, these oxides additives crystallized to intergranular glassy phase in the cooling stage [30], which deteriorate the high-temperature performance of the ceramics such as creep and high-temperature strength due to the relative low eutectic temperature [31, 35]. As a result of the early interest in hot-pressed Si_3N_4 ceramics as a high-temperature gas-turbine material, attention was directed to high-temperature strength and creep resistance. Therefore, it is quite essential to explore novel heat-resistant sintering aids for high-performance Si_3N_4 ceramics from new view point.
The last two decades have been witness to the dramatic development on MAX phase cermets with the hexagonal symmetry due to their unique combination of characteristics of both ceramics and metals (M is an early transition metal, A is a group A element, X is either carbon and/or nitrogen), especially the layered ternary carbide titanium aluminum carbide (Ti_3AlC_2) and titanium silicon carbide (Ti_3SiC_2) [36-38]. The crystal structure of these MAX cermets can be described by alternately stacking of TiC_6 and Al/Si atomic planes. The unique combination of excellent properties of Ti_3AlC_2 or Ti_3SiC_2, including high melting point, high hardness, high elastic modulus, good thermal and electrical conductivity, and considerable chemical stability, make them to be fascinating candidates for various application. Moreover, elemental metal powder-derived MAX materials have demonstrated to be effective reinforcement in TiB_2 [39-41], Al_2O_3 [42-44] composites with enhanced mechanical properties by *in situ* reaction. More recently, as explicated in our previous work [45-49], titanium aluminum carbide (Ti_3AlC_2) was chosen as an effective sintering aid to effectively densify B_4C ceramics with enhanced sintering ability and mechanical performance simultaneously. High hardness and toughness values of 28.5GPa and 7.02 $MPa{\cdot}m^{1/2}$ respectively were achieved for B_4C composites sintered with 20vol% Ti_3AlC_2 at 1900℃. The mechanisms of the enhanced sinterability of high-performance ceramics in previous works could be classified into two aspects: Firstly, the decomposed metals from Ti_3SiC_2 or Ti_3AlC_2 at high temperature can form liquid phase which promote sintering effectively. Secondly, in situ reaction sintering between matrix and titanium carbon compound would also promote densification and mechanical performance. The main competitive advantage of MAX aids is considered to be formation of reaction bonding between Si3N4 matrix and aids, rather than intergranular glassy phase. Motivated by such an idea, these non-oxides cermets are highly expected to play a multifunctional role in densification and enhancement of mechanical properties of Si_3N_4 ceramics.
It is also noteworthy that Al decomposed from Ti_3AlC_2 and residual O originated from raw Si_3N_4 powders would be dissolved into Si_3N_4 grains during high-temperature sintering procedure, which is harmful to the purity and thermal performance of Si_3N_4-based ceramics. As Y. Zhou illustrated [50], a tendency of decreasing fracture toughness with increasing Al dopant could be observed. Moreover, even the 0.4wt% concentration of Al would lead to a drastically reduce of thermal conductivity by 36.9% (from $91.9W{\cdot}m^{-1}{\cdot}K^{-1}$ to $58.0W{\cdot}m^{-1}{\cdot}K^{-1}$) for Si_3N_4 ceramics. Therefore in this work, Ti_3SiC_2 were introduced to densify Si_3N_4 ceramics in order to demonstrate that it provided any advantages over the rare-earth oxide system. Besides, the effect of

Preprints (www.preprints.org) | NOT PEER-REVIEWED | Posted: 29 February 2020 doi:10.20944/preprints202002.0464.v1

Peer-reviewed version available at Materials 2020, 13, 1428; doi:10.3390/ma13061428

Ti_3SiC_2 volume fraction on the microstructure, hardness, flexural strength and fracture toughness was also studied. It is believed that Ti_3SiC_2 or other members of MAX family would lead to new scientific and technological data providing new insight into functionalization of Si_3N_4 ceramics.

2. Experimental procedure

2.1 *Preparation of samples*

Commercially available α-Si_3N_4 powder (purity>93%, d_{50}=0.7μm, Jinshenghao New Materials Co. Ltd., China) was used as a starting material. As a novel sintering aid, Ti_3SiC_2 powders (d_{50}=5μm, purity>98%) were kindly provided by Forsman Scientific Co., Ltd., Beijing, China. In order to investigate the effect of Ti_3SiC_2 content on the mechanical properties, experiments were conducted with various amounts of Ti_3SiC_2 powders (1 to 20 vol.%) embedded in α-Si_3N_4 powders. To ensure the homogeneity of the mixed powders, α-Si_3N_4-x vol.% Ti_3SiC_2 powders (x=1~20) were wet ball-milled for 10h by using ethanol as ball-milling media. The substance was dried at 80℃, and sieved with a filter with a mesh size of 63μm, then placed in a graphite die coated with BN powder to avoid reaction between the powder and graphite die. Hot-press (HP) sintering was performed with ramp of 10℃/min 1600℃ and 1700℃ for 90min in flowing nitrogen under 30MPa uniaxial pressure during the whole cycle. After natural cooling to room temperature inside furnace, samples were polished and ultrasonic cleaned before characterization. For comparison, α-Si_3N_4 powders with 2wt.% Alumina (Al_2O_3, AR, Sinopharm Chemical Reagent Co., Ltd., China) and 5wt.% yttria (Y_2O_3, AR, Sinopharm Chemical Reagent Co., Ltd., China) were hot-pressed at the same sintering condition.

2.2 *Characterizations*

The bulk density of each sample was determined according to the Archimedes principle in distilled water. XRD patterns were recorded on X'pert PRO (PANalytical B.V., Netherlands) for phase identification. The microstructures of polished surfaces and fracture surfaces were observed using scanning electron microscopy (SEM, Nova NanoSEM230) with an energy-dispersive X-ray (EDX) analyzer. The Vickers hardness was performed on micro hardness tester (VTD 512) under load of 9.8 N with a dwell time of 10 seconds, and determined by the Vickers diamond indentation method using the following equation:

$$H_V = 0.102\frac{F}{S} = 0.102\frac{2F\sin 136/2}{d^2} = 0.1891\frac{F}{d^2} \tag{1}$$

where P is the indentation load on the polished surface and d is the average diagonal length of the Vickers indentation. For accuracy, 11 Vickers indentations on each specimen were applied. After indentation, the microstructures were immediately observed by optical microscopy (ECLISPE LV150N, Japan). As a simple way of estimating toughness, indentation techniques were applied from observed corner cracks and calculated Vickers hardness using the Anstis equation:

$$K_{IC} = 0.016\left(E/H_V\right)^{1/2}\left(P/c^{3/2}\right) \tag{2}$$

where E is the Young's modulus and c is the half-length of cracks formed by the indentation. Three-point flexural strength of specimens with size of 3mm×4mm×36mm

Preprints (www.preprints.org) | NOT PEER-REVIEWED | Posted: 29 February 2020 doi:10.20944/preprints202002.0464.v1

Peer-reviewed version available at Materials 2020, 13, 1428; doi:10.3390/ma13061428

was performed on the mechanical testing machine (Instron3369, USA) at a cross head speed of 0.5mm/min.

3. Results and discussion

Fig. 1 illustrates the density of Ti_3SiC_2 filled Si_3N_4 ceramics as a function of Ti_3SiC_2 volume fraction. For Si3N4 ceramics which HP sintered at 1600℃ without aids, the density is only 2.58 g·cm^{-3}. Partial densification may be attributed to the residual SiO_2 liquid phase during firing at high temperature which always present on Si3N4 powder particles. A remarkable increase to 3.11 g·cm^{-3} could be observed for Si_3N_4 ceramics filled with only 5vol% Ti_3SiC_2 when sintered at the same temperature. The enhanced density is even more noticeable than the Si3N4 ceramics with 7wt% Y_2O_3-Al_2O_3 aids. These observed results demonstrate Ti_3SiC_2 to be a effective sintering aid to densify Si_3N_4 ceramics. However, further increase in Ti_3SiC_2 content dose not bring any appreciable consolidation.

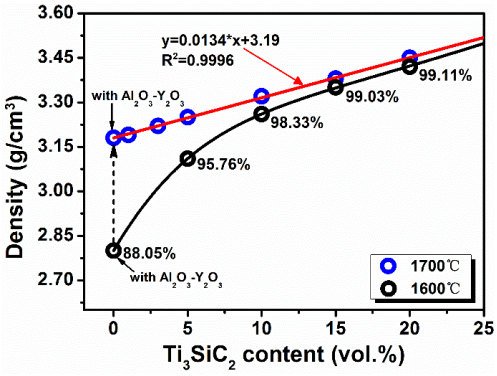

Fig. 1 Density of Si_3N_4 ceramics as a function of Ti_3SiC_2 content

As expected, higher sintering temperature 1700℃ could further promote densification of Si_3N_4 ceramics filled with Ti_3SiC_2. Besides, experimental points are inclined to distribute on a straight line with coefficient of determination (R^2) above 0.99, which is accordant with mix law. Due to the complex reaction between Si_3N_4 and Ti_3SiC_2 which will discuss later, it is difficult to determine the theoretical density of the Ti_3SiC_2-Si_3N_4 composites accurately. However, an approximation method could be applied by assuming a nearly full densification for 20vol% Ti_3SiC_2-Si_3N_4 ceramics sintered at 1700℃ according to this linear behavior.

Fig. 2 shows the XRD patterns of Si_3N_4 ceramics filled with different volume fraction of Ti_3SiC_2 sintered at 1600℃ and 1700℃, as well as 7wt% (Al_2O_3-Y_2O_3) densified Si_3N_4 ceramics. As seen in Fig. 2(a), both α and β phase of Si_3N_4 could be detected when sintering temperature is 1600℃, which suggests only a partial transformation of α phase to the more stable β phase. In contrast, when further improving sintering temperature to 1700℃, all diffraction peaks of α-Si_3N_4 phase disappear (see in Fig. 2(b)). This completely transformation of α to β-Si_3N_4 phase is believed to be essential to the enhancement of densification and mechanical performance.

Preprints (www.preprints.org) | NOT PEER-REVIEWED | Posted: 29 February 2020 doi:10.20944/preprints202002.0464.v1

Peer-reviewed version available at Materials 2020, 13, 1428; doi:10.3390/ma13061428

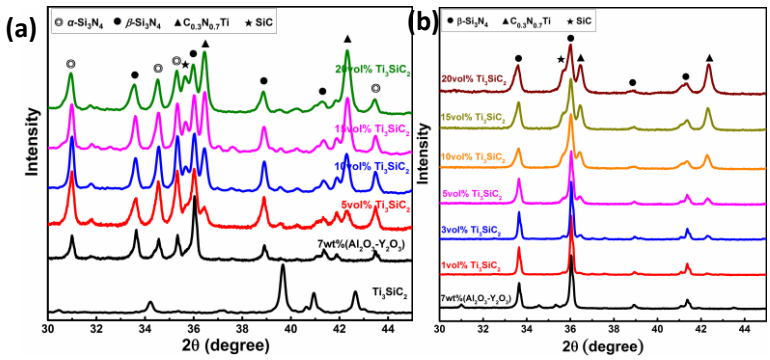

Fig. 2 XRD patterns of Ti_3SiC_2 doped Si_3N_4 ceramics sintered at (a) 1600℃ and (b) 1700℃

Another important feature should be noted here is that the characteristic diffraction peaks of the raw Ti_3SiC_2 powder nearly disappear completely after sintering. This could be ascribed to the fact that Ti_3SiC_2 powder is thermal stable up to ~800℃, and the following reaction can be responsible for the decomposition of Ti_3SiC_2 [51]:

$$3Ti_3SiC_2 \xrightarrow{\sim 800℃\ to\ 1400℃} 4TiC_x + Ti_5Si_3C_y + (6-4x-y)C \tag{3}$$

where the value of x ranges from 0.6 to 0.8 and $y \le 1$. Besides, the TiC_x phase appears to result in more rapid deterioration of the Ti_3SiC_2 phase. Also noted that the decomposition usually accomplished with decomposition of Ti_3SiC_2 to form nonstoichiometric TiC_x and gaseous Si, as demonstrated previously [52]:

$$Ti_3SiC_2 \xrightarrow{\sim 1300℃} 3TiC_{2/3} + Si \tag{4}$$

The Si is believed to be act as lubricating phase between Si_3N_4 grains to promote densification of Si_3N_4 ceramics through capillarity. Meanwhile, the residual Si would further react with nitrogen to form Si_3N_4. On the other hand, further heating during insulation stage will result in the likely loss of gaseous silicon. Furthermore, the decomposition products of Ti_3SiC_2 would further react with Si_3N_4 through diffusion of C and N according to the following reactions:

$$Ti_5Si_3C_y \longrightarrow Ti_5C_y + 3Si \tag{5}$$

$$TiC_x + Si_3N_4 \longrightarrow (3.333x-10)C_{0.3}N_{0.7}Ti + 3SiC + (5.5-1.167x)N_2 \tag{6}$$

$$Ti_5C_y + (4.5-y)C + Si_3N_4 \longrightarrow 5C_{0.3}N_{0.7}Ti + 3SiC + 0.25N_2 \tag{7}$$

$$3C + Si_3N_4 \longrightarrow 3SiC + 2N_2 \tag{8}$$

$$C + Si \longrightarrow SiC \tag{9}$$

or

$$\begin{aligned} &TiC_x + Ti_5Si_3C_y + (9.45-x-y)C + 1.55Si_3N_4 \\ &\longrightarrow 6C_{0.3}N_{0.7}Ti + 7.65SiC + N_2 \end{aligned} \tag{10}$$

It is reasonable to claim that the *in situ* reaction is responsible for the additional characteristic diffraction peaks of $C_{0.3}N_{0.7}Ti$ and SiC in XRD patterns.

Fig.3 shows the micro-morphology of polished surface of Si_3N_4 with different volume fractions of Ti_3SiC_2 sintered at 1700 ℃. Due to the lack of sufficient sintering aids, lots of pores could be observed, and grain growth of β- Si_3N_4 is not complete for monolithic Si_3N_4 ceramic (see Fig.3(a)). However, the microstructures of Ti_3SiC_2-Si_3N_4 ceramics (see Fig.3(b) to Fig.3(g)) exhibit much more close-grain

Preprints (www.preprints.org) | NOT PEER-REVIEWED | Posted: 29 February 2020 doi:10.20944/preprints202002.0464.v1

Peer-reviewed version available at Materials 2020, 13, 1428; doi:10.3390/ma13061428

structure, and consist of randomly oriented elongated Si_3N_4 grains which is accordant with XRD results in Fig.2. The average diameters of grains present slight increasing trend from 0.6771 μm to 0.9802 μm by quantitative image analysis as the amount of Ti_3SiC_2 increased. Besides, the bright contrasted phase which uniformly embedded in Si_3N_4 matrix could be observed, and are inclined to aggregate especially when Ti_3SiC_2 content exceeds 15vol%. Furthermore, as shown in Table 1, energy dispersive spectrometer (EDS) at spot A in Fig. 3(e) suggests dominant phase of Si_3N_4 and SiC, which is associated with reaction described by Eq.(10). Additional O element may be originated from surface of raw α-Si_3N_4 powders. Meanwhile, the bright region at spot B is proved to be enriched by Ti according to the EDS results in Table 1. Combined with the results of XRD analysis, it is reasonable to claim that the dispersive bright regions consist of $C_{0.3}N_{0.7}Ti$ and SiC, which are believed to affect the mechanical performance of reaction bonded Si_3N_4 ceramics.

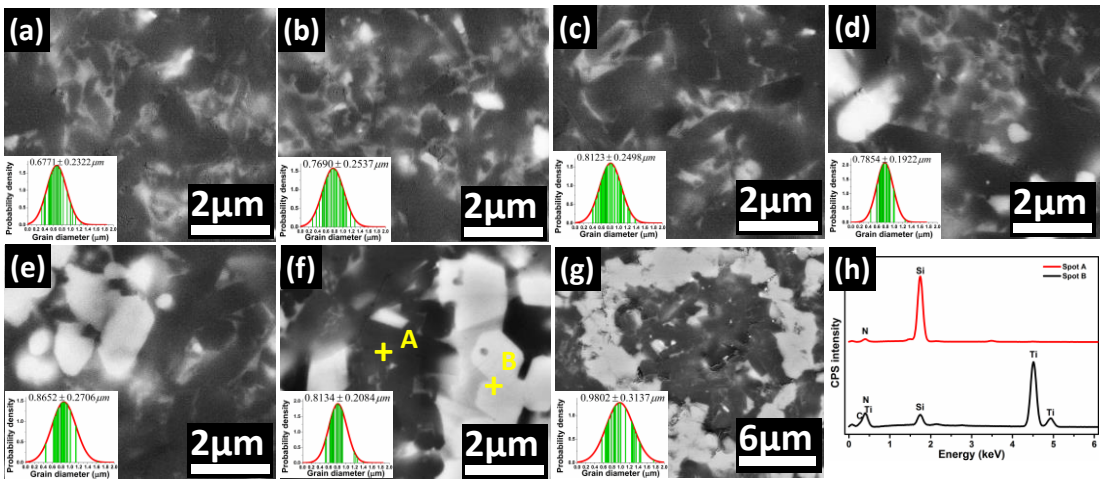

Fig. 3 Polished surface of Si_3N_4 ceramics with different content of Ti_3SiC_2 sintered at 1700℃: (a) 5wt% Y_2O_3-2wt% Al_2O_3, (b) 1vol% Ti_3SiC_2, (c) 3vol% Ti_3SiC_2, (d) 5vol% Ti_3SiC_2, (e) 10vol% Ti_3SiC_2, (f) 15vol% Ti_3SiC_2, (g) 20vol% Ti_3SiC_2, (h) EDS spectra at spot A and B

Table 1 EDS chemical analysis (at.%) at different positions in Fig. 3(g)

	Si	N	O	Ti	C	Possible phases
Spot A	52.21	35.43	2.04	1.29	9.03	Si_3N_4, SiC
Spot B	5.10	27.18	-	50.13	17.59	$C_{0.3}N_{0.7}Ti$, SiC

The mechanical properties, including Vickers hardness, flexural strength and fracture toughness, of dense Si_3N_4 ceramics with different Ti_3SiC_2 content sintered at 1700℃ are illustrated in Fig. 4. Clearly, the Vickers hardness of Si_3N_4 ceramics has been upgraded after modification of Ti_3SiC_2, and presents slight increase compared with that of Si_3N_4 ceramics containing conventional oxides aids. Besides, an obvious enhancement of flexural strength and fracture toughness could be observed. A maximum flexural strength of 795 MPa could be achieved for 5vol%Ti_3SiC_2doped Si_3N_4 composites, which is almost twice that of 7wt% (Y_2O_3-Al_2O_3)-Si_3N_4 ceramics prepared at the same condition. This enhancement of flexural strength could be attributed to the $C_{0.3}N_{0.7}Ti$ and SiC which originated from reaction bonding between Ti_3SiC_2 and Si_3N_4. However, further increment of Ti_3SiC_2 content reduces the flexural strength of Si_3N_4 ceramics which may be ascribed to the enhanced residual stresses around grain boundary. Note that this residual stress is believed to result in

Preprints (www.preprints.org) | NOT PEER-REVIEWED | Posted: 29 February 2020 doi:10.20944/preprints202002.0464.v1

Peer-reviewed version available at Materials 2020, 13, 1428; doi:10.3390/ma13061428

microcracks and intergranular fracture mode which will be discussed later. Moreover, the fracture toughness of Si_3N_4 composites is also effectively boosted after Ti_3SiC_2 decoration, and reaches maximum value of 6.97 $MPa \cdot m^{1/2}$ for 20vol%Ti_3SiC_2-Si_3N_4 ceramics which is 37% higher than that of 7wt% (Y_2O_3-%Al_2O_3)-Si_3N_4 ceramics.

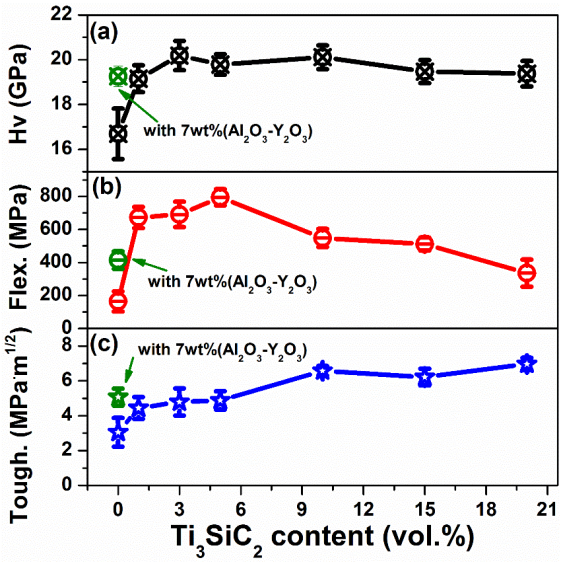

Fig. 4 Mechanical properties of Ti_3SiC_2 doped Si_3N_4 ceramics: (a) Vickers hardness, (b) flexural strength and fracture toughness

Fig. 5 illustrates the typical optical micrographs of the Vickers hardness indents and the induced cracks of Si_3N_4 ceramics with different Ti_3SiC_2 contents, as well as 7wt% (Y_2O_3-Al_2O_3). Clearly, the polished surfaces of Ti_3SiC_2 doped Si_3N_4 ceramics become much smoother than the monolithic Si_3N_4 ceramic which HP sintered at 1700℃, corresponding to the enhancement of densification. Besides, it can be seen that the area of indentation presents no obvious change for Ti_3SiC_2 doped Si_3N_4 ceramics, which is consistent with the stable Vickers hardness. However, the cracks obviously become shorter especially when the Ti_3SiC_2 contents exceed 10vol%, which is responsible for the enhancement of fracture toughness.

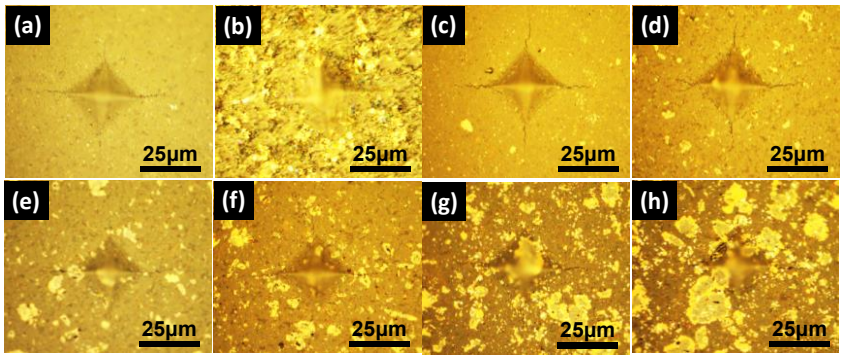

Fig. 5 Optical micrographs of the Vickers hardness indents and the induced cracks in (a) Si_3N_4-7wt% (Al_2O_3-Y_2O_3), (b) Si_3N_4-3vol% Ti_3SiC_2, (c) Si_3N_4-5vol% Ti_3SiC_2, (d) Si_3N_4-10vol% Ti_3SiC_2, (e) Si_3N_4-15vol% Ti_3SiC_2, (f) Si_3N_4-20vol% Ti_3SiC_2

To illustrate the fracture behaviors and activated toughening mechanisms, micromorphology and crack paths are investigated on cross-sectional fracture surfaces and polished surfaces, respectively. Comparison of typical fracture surfaces between

Preprints (www.preprints.org) | NOT PEER-REVIEWED | Posted: 29 February 2020 doi:10.20944/preprints202002.0464.v1

Peer-reviewed version available at Materials 2020, 13, 1428; doi:10.3390/ma13061428

Si_3N_4 doped with Al_2O_3-Y_2O_3 and Ti_3SiC_2 is illustrated in Fig. 6. As can be seen from Fig. 6(a), a small amount of pores occur in the Si_3N_4-7wt% (Al_2O_3-Y_2O_3) composites, which is harmful for the mechanical performances. In contrast, the Si_3N_4-Ti_3SiC_2 specimen presents a much more close-grain fracture surface owning to the higher density. As marked by red arrows in Fig. 6(b), large amounts of dimples corresponding to the transgranular fracture could be observed. And this fracture mode is considered to make a dominate contribution to the superior flexural strength of Si_3N_4-Ti_3SiC_2 composites. Besides, as marked by yellow arrows, lots of interface debonding between the Si_3N_4 grains and grain boundary phase could be observed. This intergranular fracture mode may result from the pullout of elongated β-Si_3N_4 grains, which is believed to make a contribution to the enhancement of overall fracture toughness.

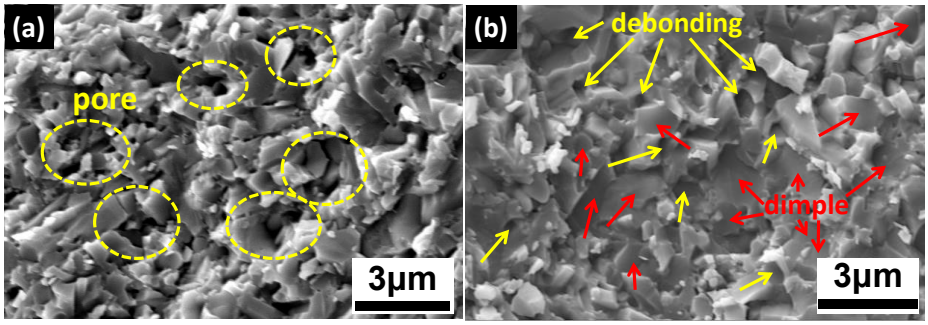

Fig. 6 Typical fracture surfaces of Si_3N_4 with (a) 7wt% (Al_2O_3-Y_2O_3), (b) 10vol% Ti_3SiC_2

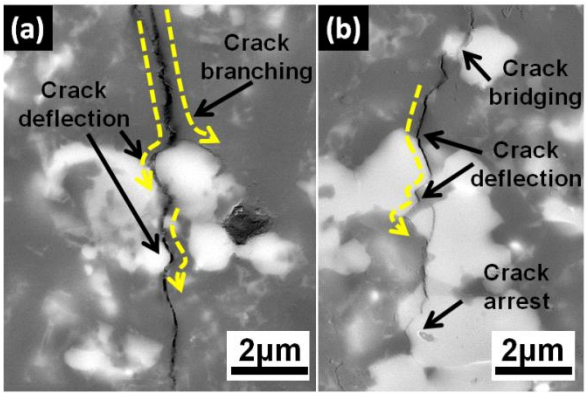

Fig. 7 Typical SEM images of crack deflection in Ti_3SiC_2 densified Si_3N_4 composites

Another mechanism of the enhanced fracture toughness of Si_3N_4-Ti_3SiC_2 composites could be ascribed to the crack branching, deflection and grain bridging by *in-situ* derived $C_{0.3}N_{0.7}Ti$ and SiC grains embedded in Si_3N_4 matrix, which illustrated in Fig. 7. Due to the superior hardness of $C_{0.3}N_{0.7}Ti$ and the thermal mismatch between Si_3N_4 and $C_{0.3}N_{0.7}Ti$, there exists residual stress around $C_{0.3}N_{0.7}Ti$ grains during cooling, giving rise to the microcracks inside composites. When subjected to the external mechanical stress, these microcracks tend to be activated and the propagation path of cracks tends to be splitted by $C_{0.3}N_{0.7}Ti$ hard-phase and deflected along the interface. Such mechanisms consumed more fracture energy during the crack propagation which leads to crack arrest.

A comparison of mechanical properties of Si_3N_4-based ceramics obtained in the present work and selected previous works with conventional oxide aids is shown in Table 2.

Preprints (www.preprints.org) | NOT PEER-REVIEWED | Posted: 29 February 2020 doi:10.20944/preprints202002.0464.v1

Peer-reviewed version available at Materials 2020, 13, 1428; doi:10.3390/ma13061428

Clearly, the Vickers , flexural strength and toughness of Ti_3SiC_2 doped Si_3N_4 ceramics present the same level or even better compared with Si_3N_4 ceramics sintered with oxide aids. Moreover, due to the superior mechanical and thermal properties of *in situ* formed $C_{0.3}N_{0.7}Ti$ and SiC, Si_3N_4 ceramics obtained in this work are believed to have a significant competitive advantage and to promote the development of Si_3N_4-based ceramics at high temperatures.

Table 2 Selected results on mechanical properties of Si_3N_4 ceramics by pressure-assisted sintering

Composition	Sintering conditions	Vickers hardness (GPa)	Flexural strength (MPa)	Fracture toughness (MPa.m1/2)	Ref.
α -Si_3N_4+4wt% Al_2O_3+6wt% Y_2O_3	Hot isostatic pressing at 1700℃, 20MPa, 3h	16.4	730	6.5	[26]
α - Si_3N_4+5wt% Al_2O_3+5wt% Y_2O_3	Hot press at 1800℃, 30MPa, 1.5h	16.1	-	5.2	[19]
α - Si_3N_4+4wt% Al_2O_3+6wt% Y_2O_3	Hot press at 1700℃, 50MPa, 1.5h	17.01	-	-	[20]
α - Si_3N_4+30vol% β - Si_3N_4 whiskers+5wt% Al_2O_3+5wt% Y_2O_3+5wt% CeO_2	Hot press at 1700℃, 30MPa, 30min	19.0	794	8.6	[21]
α - Si_3N_4+4wt% Al_2O_3+4wt% Y_2O_3+15vol% SiC whiskers	Hot press at 1800℃, 30MPa, 30min	16	680	6.1	[53]
α - Si_3N_4+5wt% Al_2O_3+4wt% Y_2O_3+3wt% TiC	Gas pressure sintering at 1750℃, 2MPa	16.4	475	7.6	[10]
α - Si_3N_4+5vol% Ti_3SiC_2	Hot-pressed at 1700℃ for 90min	19.78	795	4.88	This work
α - Si_3N_4+20vol% Ti_3SiC_2	Hot-pressed at 1700℃ for 90min	20.11	549	6.58	This work

4. Conclusions

In summary, we proposed non-oxide Ti_3SiC_2 (one of typical MAX cermets) as a novel sintering aid to densify Si_3N_4 ceramics with enhanced mechanical properties. A remarkable relative density increment of 20.5% (from 2.58 to 3.11 $g \cdot cm^{-3}$) could be observed for 1600℃ hot-presssinteredSi_3N_4 ceramics doped with only 5vol% Ti_3SiC_2 compared with Si_3N_4 ceramics without aids. Further increase in sintering temperature to 1700℃ brought appreciable consolidation of nearly full dense Ti_3SiC_2-Si_3N_4 ceramics. XRD and EDS investigations demonstrated the formation of $C_{0.3}N_{0.7}Ti$ and SiC which resulted from *in-situ* reaction between $Ti_3SiC_2$and Si_3N_4 through diffusion of C and N. The Vickers hardness of Ti_3SiC_2 doped Si_3N_4 ceramics increased slight compared with that of Si_3N_4 ceramics containing conventional oxides aids. Nevertheless, an obvious enhancement of flexural strength and fracture toughness could be observed. A maximum flexural strength of 795 MPa could be obtained for 5vol%Ti_3SiC_2 doped Si_3N_4 composites. Moreover, the fracture toughness of Ti_3SiC_2 densified Si_3N_4 composites exhibited a remarkable increase with increasing in volume fraction, and reached maximum value of 6.97 $MPa \cdot m^{1/2}$ for 20vol% Ti_3SiC_2-Si_3N_4 ceramics. Pull out of elongated Si_3N_4 grains, crack bridging and deflection were demonstrated to promote fracture toughness of Ti_3SiC_2 densified Si_3N_4 composites. With these successes, MAX phase densified Si_3N_4 ceramics with enhanced strength and toughness will be necessary to meet demands of potential future markets for

advanced ceramics. Further efforts are encouraged to be devoted to thermal properties investigations of MAX enabled Si_3N_4 composites.

Acknowledgements

This work was supported by the National Key Research and Development Program of China(Grant No. 2017YFA0204600), the National Natural Science Foundation of China (Grant No. 51802352), the China Postdoctoral Science Foundation (Grant No. 2017M612996).

References

1. Xu, W., et al., Effects of sintering additives on mechanical properties and microstructure of Si3N4 ceramics by microwave sintering. Materials Science and Engineering: A, 2017. **684**:127-134.DOI:http://dx.doi.org/10.1016/j.msea.2016.12.031
2. Kandi, K.K., N. Thallapalli, and S.P.R. Chilakalapalli, Development of Silicon Nitride-Based Ceramic Radomes — A Review. International Journal of Applied Ceramic Technology, 2015. **12**(5):909–920
3. Nishimura, T., et al., Fabrication of silicon nitride nanoceramics—Powder preparation and sintering: A review. Science and Technology of Advanced Materials, 2007. **8**(7–8):635-643.DOI:http://dx.doi.org/10.1016/j.stam.2007.08.006
4. Luo, H., et al., Modeling for high-temperature dielectric behavior of multilayer Cf/Si3N4 composites in X-band. Journal of the European Ceramic Society, 2017. **37**(5):1961-1968.DOI:http://dx.doi.org/10.1016/j.jeurceramsoc.2016.12.028
5. Bucio, T.D., et al., Silicon Nitride Photonics for the Near-Infrared. Ieee Journal of Selected Topics in Quantum Electronics, 2020. **26**(2):13.DOI:10.1109/jstqe.2019.2934127
6. Wen, Z.L., et al., Investigation on Electromagnetic Wave Absorption of SiCw/Si3N4 Composites Exposed to Short-Time Oxidation. Journal of Nanoscience and Nanotechnology, 2020. **20**(3):1859-1865.DOI:10.1166/jnn.2020.17337
7. Kiani, K.M., et al., Thulium-doped tellurium oxide waveguide amplifier with 7.6dB net gain on a silicon nitride chip. Optics letters, 2019. **44**(23):5788-5791.DOI:10.1364/ol.44.005788
8. Zanocco, M., et al., The role of nitrogen off-stoichiometry in the osteogenic behavior of silicon nitride bioceramics. Materials Science & Engineering C-Materials for Biological Applications, 2019. **105**:8.DOI:10.1016/j.msec.2019.110053
9. Nikonam, M.R., M.D. Pugh, and R.A.L. Drew, Microstructural evolution mechanism of porous reaction bonded silicon nitride ceramics heat-treated in two powder beds. Ceramics International, 2019. **45**(17):21986-21997.DOI:10.1016/j.ceramint.2019.07.213
10. Ye, C., et al., Effect of addition of micron-sized TiC particles on mechanical properties of Si3N4 matrix composites. Journal of Alloys and Compounds, 2017. **709**:165-171.DOI:http://dx.doi.org/10.1016/j.jallcom.2017.03.124
11. Bocanegra-Bernal, M.H. and B. Matovic, Mechanical properties of silicon nitride-based ceramics and its use in structural applications at high temperatures. Materials Science and Engineering: A, 2010. **527**(6):1314-1338.DOI:http://dx.doi.org/10.1016/j.msea.2009.09.064
12. Klemm, H., Silicon Nitride for High-Temperature Applications. Journal of the American Ceramic Society, 2010. **93**(6):1501-1522.DOI:10.1111/j.1551-2916.2010.03839.x
13. Shi, C., et al., Fabrication of silicon nitride fiber-PMMA composite through free radical polymerization in batch. Materials Research Bulletin, 2014. **51**:161-166.DOI:10.1016/j.materresbull.2013.12.010
14. Eblagon, F., et al., Development of silicon nitride/silicon carbide composites for wood-cutting tools. Journal of the European Ceramic Society, 2007. **27**(1):419-428
15. buzbee, m., et al. Silicon nitride on-silicon 3-dimensional photonic circuits for integrated photodetection. in *Advanced Photonics 2016 (IPR, NOMA, Sensors, Networks, SPPCom, SOF)*. 2016. Vancouver: Optical Society of America.
16. Xie, W., et al., On-Chip Integrated Quantum-Dot–Silicon-Nitride Microdisk Lasers. Advanced Materials, 2017. **29**(16):1604866-6.DOI:10.1002/adma.201604866
17. Nishiyama, N., et al., Transparent polycrystalline cubic silicon nitride. Scientific Reports, 2017. **7**:44755
18. Capelle, T., et al., Polarimetric analysis of stress anisotropy in nanomechanical silicon

nitride resonators. Applied Physics Letters, 2017. **110**(18):103125-1305

19. Yu, J.-J., et al., Graded Si 3 N 4 ceramics with hard surface and tough core by two-step hot pressing. Ceramics International, 2017. **43**(10):7948-7950.DOI:10.1016/j.ceramint.2017.03.089
20. Balázsi, C., et al., Si 3 N 4 /graphene nanocomposites for tribological application in aqueous environments prepared by attritor milling and hot pressing. Journal of the European Ceramic Society, 2017. **37**(12):3797-3804.DOI:10.1016/j.jeurceramsoc.2017.03.022
21. Xing, H., et al., Mechanical properties of Si3N4 ceramics from an in-situ synthesized a-Si3N4/β-Si3N4 composite powder. Ceramics International, 2017. **43**(2):2150-2154.DOI:http://dx.doi.org/10.1016/j.ceramint.2016.10.196
22. Liang, H., et al., Mechanical properties and thermal conductivity of Si3N4 ceramics with YF3 and MgO as sintering additives. Ceramics International, 2016. **42**(14):15679-15686.DOI:http://dx.doi.org/10.1016/j.ceramint.2016.07.024
23. Li, S., et al., Sintering of High - Performance Silicon Nitride Ceramics Under Vibratory Pressure. Journal of the American Ceramic Society, 2015. **98**(3):698-701
24. Mikijelj, B., et al., Intergranular Nanostructure Effects on Strength and Toughness of Si3N4. Journal of the American Ceramic Society, 2015. **98**(5):1650-1657
25. Zhou, M.Y., et al., Microstructures and properties of Si3N4/TiN composites sintered by hot pressing and spark plasma sintering. Materials Research Bulletin, 2013. **48**(5):1927-1933.DOI:10.1016/j.materresbull.2013.01.045
26. Kovalčíková, A., et al., Influence of hBN content on mechanical and tribological properties of Si3N4/BN ceramic composites. Journal of the European Ceramic Society, 2014. **34**(14):3319-3328.DOI:http://dx.doi.org/10.1016/j.jeurceramsoc.2014.02.021
27. Shen, Z., et al., Formation of tough interlocking microstructures in silicon nitride ceramics by dynamic ripening. Nature, 2002. **417**(6886):266
28. Ahmad, N. and H. Sueyoshi, Microstructure and mechanical properties of silicon nitride-titanium nitride composites prepared by spark plasma sintering. Materials Research Bulletin, 2011. **46**(3):460-463.DOI:10.1016/j.materresbull.2010.11.021
29. Chockalingam, S. and D.A. Earl, Mechanical properties of 2.45GHz microwave sintered Si3N4–Y2O3–MgO–ZrO2 system. Journal of the European Ceramic Society, 2009. **29**(10):2037-2043.DOI:http://dx.doi.org/10.1016/j.jeurceramsoc.2009.01.006
30. Shibata, N., et al., Observation of rare-earth segregation in silicon nitride ceramics at subnanometre dimensions. Nature, 2004. **428**(6984):730-733
31. Riley, F.L., Silicon Nitride and Related Materials. Journal of the American Ceramic Society, 2010. **83**(2):245-265
32. Lojanová, S., et al., Rare-earth element doped Si3N4/SiC micro/nano-composites—RT and HT mechanical properties. Journal of the European Ceramic Society, 2010. **30**(9):1931-1944.DOI:http://dx.doi.org/10.1016/j.jeurceramsoc.2010.03.007
33. Guo, W.-M., et al., Rapid fabrication of Si3N4 ceramics by reaction-bonding and pressureless sintering. Journal of the European Ceramic Society, 2016. **36**(16):3919-3924.DOI:http://dx.doi.org/10.1016/j.jeurceramsoc.2016.06.007
34. Luo, H., P. Xiao, and W. Hong, Dielectric behavior of laminate-structure Cf/Si3N4 composites in X-band. Applied Physics Letters, 2014. **105**(17):172903.DOI:10.1063/1.4900932
35. Park, H., H.-E.K. †, and K. Niihara, Microstructural Evolution and Mechanical Properties of Si 3 N 4 with Yb 2 O 3 as a Sintering Additive. Journal of the American Ceramic Society, 1997. **80**(3):750–756
36. Barsoum, M.W., The M N+1AX N phases: A new class of solids. Progress in Solid State Chemistry, 2000. **28**(1):201-281
37. Sun, Z.M., Progress in research and development on MAX phases: a family of layered ternary compounds. International Materials Reviews, 2011. **56**(3):143-166
38. Tzenov, N.V. and M.W. Barsoum, Synthesis and Characterization of Ti3AlC2. Journal of the American Ceramic Society, 2010. **83**(4):825-832
39. Zhou, W., B. Mei, and J. Zhu, Rapid synthesis of Ti 3 AlC 2 /TiB 2 composites by the spark plasma sintering (SPS) technique. Ceramics International, 2009. **35**(8):3507-3510
40. Li, M., et al., Oxidation Behavior of a Ti3AlC2/TiB2 Composite at 1000°–1400°C in Air. Journal of the American Ceramic Society, 2010. **93**(2):554-560

41. Li, C., et al., In Situ Synthesis and Properties of Ti 3 AlC 2 /TiB 2 Composites. Journal of the American Ceramic Society, 2007. **90**(11):3615–3620
42. Zhu, J., L. Ye, and F. Wang, Fabrication of Ti3AlC2/Al2O3 nanocomposite by a novel method. Science of Sintering, 2011. **43**(3):289-294
43. Yeh, C.L., C.W. Kuo, and Y.C. Chu, Formation of Ti 3 AlC 2 /Al 2 O 3 and Ti 2 AlC/Al 2 O 3 composites by combustion synthesis in Ti–Al–C–TiO 2 systems. Journal of Alloys & Compounds, 2010. **494**(s 1–2):132–136
44. Liu, Y., et al., Mechanical, Dielectric, and Microwave-Absorption Properties of Alumina Ceramic Containing Dispersed Ti 3 SiC 2. Journal of Electronic Materials, 2015. **44**(3):867-873
45. Tan, Y.Q., et al., Enhancement of sinterability and mechanical properties of B4C ceramics using Ti3AlC2 as a sintering aid. Rsc Advances, 2015. **5**(93):76309-76314
46. Tan, Y., et al., Lightweight graphene nanoplatelet/boron carbide composite with high EMI shielding effectiveness. AIP Advances, 2016. **6**(3):035208.DOI:doi:http://dx.doi.org/10.1063/1.4943977
47. Tan, Y., et al., Fabrication of toughened B4C composites with high electrical conductivity using MAX phase as a novel sintering aid. Ceramics International, 2016. **42**(6):7347-7352.DOI:10.1016/j.ceramint.2016.01.133
48. Tan, Y., et al., Graphene nanoplatelet reinforced boron carbide composites with high electrical and thermal conductivity. Journal of the European Ceramic Society, 2016. **36**(11):2679-2687.DOI:10.1016/j.jeurceramsoc.2016.04.036
49. Tan, Y., H. Zhang, and S. Peng, Electrically conductive graphene nanoplatelet/boron carbide composites with high hardness and toughness. Scripta Materialia, 2016. **114**:98-102.DOI:http://dx.doi.org/10.1016/j.scriptamat.2015.12.008
50. Zhou, Y., et al., Development of high-thermal-conductivity silicon nitride ceramics. Journal of Asian Ceramic Societies, (0).DOI:http://dx.doi.org/10.1016/j.jascer.2015.03.003
51. Wu, E., et al., In Situ Neutron Powder Diffraction Study of Ti3SiC2 Synthesis. Journal of the American Ceramic Society, 2004. **84**(10):2281-2288
52. Racault, C., F. Langlais, and R. Naslain, Solid-state synthesis and characterization of the ternary phase Ti 3 SiC 2. Journal of Materials Science, 1994. **29**(13):3384-3392
53. Wu, W., et al., Si3N4-SiCw composites as structural materials for cryogenic application. Journal of the European Ceramic Society, 2016. **36**(11):2667-2672.DOI:http://dx.doi.org/10.1016/j.jeurceramsoc.2016.04.019